

Article

Hydrothermal CO₂ Reduction by Glucose as Reducing Agent and Metals and Metal Oxides as Catalysts

Maira I. Chinchilla , Fidel A. Mato, Ángel Martín and María D. Bermejo  *

High Pressure Process Group, Department of Chemical Engineering and Environmental Technology, BioEcoUva Research Institute on Bioeconomy, Universidad de Valladolid, 47011 Valladolid, Spain; mairaivette.chinchilla@alumnos.uva.es (M.I.C.); fidel@iq.uva.es (F.A.M.); mamaan@iq.uva.es (Á.M.)

* Correspondence: mdbermejo@iq.uva.es

Abstract: High-temperature water reactions to reduce carbon dioxide were carried out by using an organic reductant and a series of metals and metal oxides as catalysts, as well as activated carbon (C). As CO₂ source, sodium bicarbonate and ammonium carbamate were used. Glucose was the reductant. Cu, Ni, Pd/C 5%, Ru/C 5%, C, Fe₂O₃ and Fe₃O₄ were the catalysts tested. The products of CO₂ reduction were formic acid and other subproducts from sugar hydrolysis such as acetic acid and lactic acid. Reactions with sodium bicarbonate reached higher yields of formic acid in comparison to ammonium carbamate reactions. Higher yields of formic acid (53% and 52%) were obtained by using C and Fe₃O₄ as catalysts and sodium bicarbonate as carbon source. Reactions with ammonium carbamate achieved a yield of formic acid up to 25% by using Fe₃O₄ as catalyst. The origin of the carbon that forms formic acid was investigated by using NaH¹³CO₃ as carbon source. Depending on the catalyst, the fraction of formic acid coming from the reduction of the isotope of sodium bicarbonate varied from 32 to 81%. This fraction decreased in the following order: Pd/C 5% > Ru/C 5% > Ni > Cu > C ≈ Fe₂O₃ > Fe₃O₄.

Keywords: hydrothermal reaction; CO₂ conversion; glucose; metal catalysts; metal oxide catalysts



Citation: Chinchilla, M.I.; Mato, F.A.;

Martín, Á.; Bermejo, M.D.

Hydrothermal CO₂ Reduction by Glucose as Reducing Agent and Metals and Metal Oxides as Catalysts.

Molecules **2022**, *27*, 1652.

<https://doi.org/10.3390/molecules27051652>

Academic Editors: Reza Haghbakhsh, Sona Raeissi and Rita Craveiro

Received: 31 January 2022

Accepted: 1 March 2022

Published: 2 March 2022

Publisher's Note: MDPI stays neutral with regard to jurisdictional claims in published maps and institutional affiliations.



Copyright: © 2022 by the authors. Licensee MDPI, Basel, Switzerland. This article is an open access article distributed under the terms and conditions of the Creative Commons Attribution (CC BY) license (<https://creativecommons.org/licenses/by/4.0/>).

1. Introduction

Global warming is still one of the main worldwide concerns in the present time [1,2]. Increasing the efficiency of processes, implementing renewable sources of energy and fuel switching are some of the alternatives for the reduction of greenhouse emissions [3]. However, in the transition to a decarbonated economy, oil and gas still play a relevant role in energy generation for electricity and transportation; in this context, technological initiatives as carbon capture and utilization become of high interest to mitigate these emissions by using CO₂ to synthesize high value-added products [4].

CO₂ is attractive as a raw material for industry because it is cheap, has very low toxicity, is available in great quantity [5] and can be used as feedstock for different processes. Physical methods are widely used to revalorize CO₂ as refrigerant, solvent, dry ice, etc. Chemical methods are also used to convert it into valuable compounds such as urea and DME [6,7]. One of the main difficulties faced in the chemical conversion of CO₂ is the high thermodynamic stability of the compound [8]. Electrochemical and photochemical reduction for CO₂ hydrogenation have shown favorable results in overcoming this issue [9]. However, the high costs and low yields of these techniques [10] have led to the study of other alternatives such as the hydrothermal treatment in which CO₂ reduction takes place in water media at high pressures and temperatures [11–13]. In this process, water acts as hydrogen donor instead of H₂, which is flammable and complex to store [14].

In these processes, CO₂ is captured in the aqueous media in basic conditions. In most works, it is captured as NaHCO₃, but it can be also in the shape of carbamates that are formed when CO₂ is captured by ammonia or amines. This process opens the possibility

to connect carbon capture in basic solutions directly with the CO₂ conversion process, avoiding costly intermediate separation steps [12,15].

In the hydrothermal reduction of CO₂, the most frequently obtained product is formic acid. This is a compound of great interest for the energy sector because it is an alternative source of hydrogen and can be used directly as an energy-dense carrier for fuel cells [16]; besides, it is biodegradable and less flammable than other fuels at room temperature [17].

In order to reduce CO₂, several metals have been suggested as CO₂ reductants: Zn [18], Fe [19], Mn [20], Mg [20] and Al [20] (efficiency: Al > Zn > Mn > Fe) [10,21] are mentioned as favorable for the process. Metallic catalysts metals such as Ni-ferrite [22], Ni nanoparticles [23], Ni [24], Raney Ni [25], Cu [20,21], Fe₂O₃ [26], Ru/C [27] and Pd/C [12,27] can be used as-is or coupled with “zero-valent” metals to improve the reaction; however, the reduction of the metal after the process in order to recycle the material should be considered.

Organic compounds containing alcohol groups, such as isopropanol [8], glycerol [28], glucose, C2 and C3 alcohols, saccharides and lignin derivatives [29], are often used as reductants as well. It is known that many of these molecules can be obtained from the hydrolysis of lignocellulosic biomass in hydrothermal media.

Subcritical water can act as a basic or acidic catalyst; it has a higher ion product and lower dielectric constant than room-temperature water. In these conditions, the cellulose, hemicellulose and lignin from biomass can be isolated and depolymerized into monomeric units (mainly sugars or phenols). Alongside the decarbonization approach, the usage of biomass is of great interest mainly because of the valorization of lignocellulosic residues that can be converted into several intermediate products such as lactic acid, acetic acid and vanillin [30,31]. Carrying out the hydrolysis of biomass simultaneously with the reduction of CO₂ captured as a basic solution (i.e., bicarbonate, amine carbamates of ammonia) could be interesting because many of the hydrolysis products of biomass contain alcohol groups that can act as reductants of CO₂ in hydrothermal media.

So far, there has been a number of studies in which the use of catalysts (Cu, Ni, Pd/C) in hydrothermal CO₂ reduction was carried out using metals as reductants (Zn, Mg, Al, etc.) [12,18,20–22,25]. This work studies, for the first time, the influence of different catalysts in the hydrothermal reduction of CO₂ by using an organic (glucose) as a reducing agent. As CO₂ source, sodium bicarbonate (NaHCO₃) and ammonium carbamate (NH₄[H₂NCO₂]) were used. There are literature studies stating that ammonium carbamate is reduced by using metals or hydrogen [12], but this is the first time that the reduction is performed using organics containing an alcohol group. The main objective of the present work is to develop batch screening reactions to find the best catalyst that can improve the formic acid production, as well as lowering the temperature for the reduction reactions normally fixed at 300 °C in other works [29]. In addition, as formic acid can be also derived by sugar hydrolysis [32–35], experiments to study the origin of the carbon forming formic acid by using NaH¹³CO₃ as carbon source were performed.

2. Results

To perform the reduction of CO₂, several experiments were carried out by using glucose as organic reductant, sodium bicarbonate (SB) and ammonium carbamate (AC) as sources of carbon and several metals and metal oxides as catalysts (Cu, Ni, Pd/C 5%, Ru/C 5%, Fe₂O₃ and Fe₃O₄). Activated carbon (C) was used in some experiments in order to compare its performance with the palladium and ruthenium supported catalysts.

It should be noted that only the products of the liquid phase were analyzed. Gas products were not formed or were produced in so small amounts that they could not be collected. It is not excluded that gases such as CH₄ [23,24] could be produced in a very small amount in the case of Ni catalyst.

2.1. Particle Size of the Catalysts

As seen in Figure 1, SEM images of the unreacted catalysts were taken in order to measure the average particle size. The approximate diameters of the particles of each the catalysts before the hydrothermal reaction were as follows: Cu: 400 μm ; Ni: 9 μm ; Pd/C: 25 μm ; C: 55 μm ; Ru/C: 175 μm ; Fe_2O_3 ; Fe_3O_4 : 93 μm .

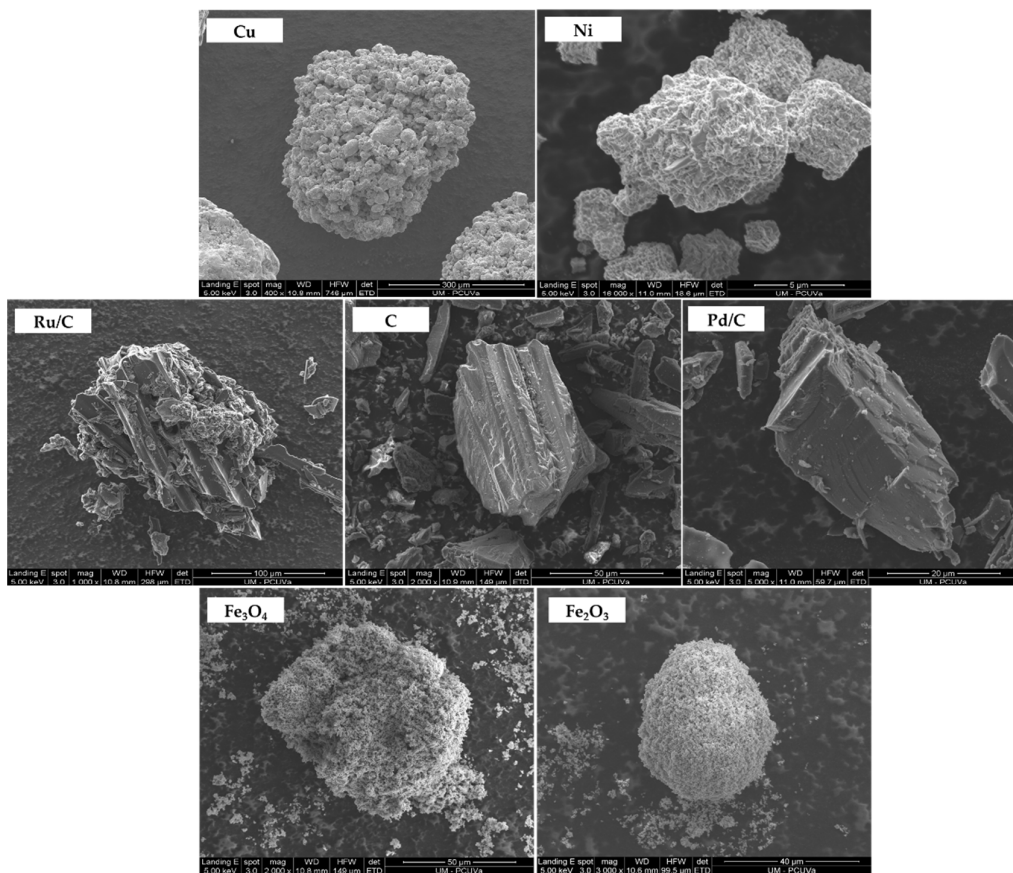


Figure 1. SEM images of the catalyst particles.

2.2. Results of Hydrothermal Reactions with Sodium Bicarbonate as Carbon Source

In the reaction of SB with glucose, typical products derived from the hydrothermal reduction of glucose were observed [29,33–37]. Formic acid (FA), acetic acid (AA) and lactic acid (LA) were the main compounds produced in the reactions. In minor amounts, glyceraldehyde, glycolaldehyde, formaldehyde, ethylene glycol, acetone, pyruvaldehyde, galacturonic acid and 5-HMF were obtained. The yields of the three main products of the catalyzed reactions are shown in Tables 1–3. Each experiment was repeated at least twice, the average error being around 5%.

After carrying out the reduction of CO_2 captured as SB, it was found that the highest yields of FA were obtained by using C and Fe_3O_4 as catalysts, reaching yields of 53% and 52%, respectively (Table 1). The conditions at which the maximum values were obtained were 200 $^{\circ}\text{C}$ and 30 min of reaction for C and 250 $^{\circ}\text{C}$ and 30 min of reaction for Fe_3O_4 .

The highest yield for AA was obtained in the sample without catalyst: 45% at 250 $^{\circ}\text{C}$ and 30 min. This was followed by Ni and Cu catalysts, which achieved yields of 45% and 44%, at 250 $^{\circ}\text{C}$ and 30 min and 250 $^{\circ}\text{C}$ and 120 min (Table 2).

For LA, the maximum yield was achieved with Fe_3O_4 , 43% at 250 $^{\circ}\text{C}$ and 30 min of reaction (Table 3).

It is remarkable that most of the catalysts promoted similar or less yield of FA in comparison to the sample without catalyst; in fact, only C and Fe_3O_4 improved the yield of FA over AA and LA over the sample with no catalyst.

Table 1. Yields of formic acid obtained after the hydrothermal reaction of NaHCO_3 with glucose in the presence of catalysts. The higher yields obtained after the hydrothermal reactions are marked with an asterisk (*).

Reaction Time (min)	Reaction Temperature: 200 °C								No Catalyst
	Cu	Ni	Pd/C	C	Ru/C	Fe_3O_4	Fe_2O_3		
30	44%	44%	20%	* 53%	31%	49%	45%	44%	
60	43%	40%	16%	46%	30%	51%	49%	48%	
90	43%	35%	18%	51%	25%	48%	45%	-	
120	39%	34%	20%	51%	27%	49%	48%	51%	
180	39%	32%	20%	37%	23%	46%	41%	40%	

Reaction Time (min)	Reaction Temperature: 250 °C								No Catalyst
	Cu	Ni	Pd/C	C	Ru/C	Fe_3O_4	Fe_2O_3		
30	41%	41%	29%	50%	38%	* 52%	40%	47%	
60	36%	-	31%	47%	33%	44%	42%	41%	
90	37%	35%	36%	47%	31%	44%	39%	38%	
120	37%	40%	35%	46%	32%	49%	40%	40%	
180	32%	34%	38%	46%	26%	45%	40%	39%	

Table 2. Yields of acetic acid obtained after the hydrothermal reaction of NaHCO_3 with glucose in the presence of catalysts. The higher yields obtained after the hydrothermal reactions are marked with an asterisk (*).

Reaction Time (min)	Reaction Temperature: 200 °C								No Catalyst
	Cu	Ni	Pd/C	C	Ru/C	Fe_3O_4	Fe_2O_3		
30	39%	40%	25%	33%	31%	31%	38%	39%	
60	38%	41%	26%	33%	33%	33%	39%	40%	
90	40%	39%	23%	34%	35%	35%	39%	40%	
120	38%	37%	27%	33%	31%	31%	37%	37%	
180	36%	36%	27%	28%	31%	31%	37%	37%	

Reaction Time (min)	Reaction Temperature: 250 °C								No Catalyst
	Cu	Ni	Pd/C	C	Ru/C	Fe_3O_4	Fe_2O_3		
30	40%	* 45%	26%	33%	34%	34%	41%	* 45%	
60	-	-	23%	30%	27%	27%	-	38%	
90	43%	42%	24%	35%	30%	30%	39%	38%	
120	* 44%	43%	24%	35%	30%	30%	39%	-	
180	37%	39%	24%	34%	30%	30%	39%	40%	

Table 3. Yields of lactic acid obtained after the hydrothermal reaction of NaHCO_3 with glucose in the presence of catalysts. The higher yields obtained after the hydrothermal reactions are marked with an asterisk (*).

Reaction Time (min)	Reaction Temperature: 200 °C							
	Cu	Ni	Pd/C	C	Ru/C	Fe_3O_4	Fe_2O_3	No Catalyst
30	34%	34%	23%	28%	33%	35%	35%	35%
60	31%	31%	22%	26%	32%	34%	34%	34%
90	36%	31%	27%	29%	30%	37%	37%	36%
120	32%	32%	27%	-	29%	34%	34%	34%
180	31%	33%	28%	34%	28%	33%	31%	31%

Reaction Time (min)	Reaction Temperature: 250 °C							
	Cu	Ni	Pd/C	C	Ru/C	Fe_3O_4	Fe_2O_3	No Catalyst
30	35%	38%	36%	39%	39%	* 43%	37%	38%
60	33%	-	33%	40%	32%	40%	40%	35%
90	36%	38%	39%	39%	34%	35%	40%	35%
120	34%	39%	34%	38%	34%	38%	37%	38%
180	31%	37%	31%	36%	29%	36%	34%	37%

Results of Hydrothermal Reactions with Ammonium Carbamate as Carbon Source

As in the previous case, the main products of the reaction with AC were FA, AA and LA. The yields achieved for each compound are shown in Tables 4–6. The experiments were repeated at least twice, the average error being around 3%.

Table 4. Yields of formic acid obtained after the hydrothermal reaction of $\text{NH}_4[\text{H}_2\text{NCO}_2]$ with glucose in the presence of catalysts. The higher yields obtained after the hydrothermal reactions are marked with an asterisk (*).

Reaction Time (min)	Reaction Temperature: 200 °C							
	Cu	Ni	Pd/C	C	Ru/C	Fe_3O_4	Fe_2O_3	No Catalyst
30	16%	14%	9%	21%	9%	21%	18%	17%
60	17%	19%	7%	-	-	20%	17%	17%
90	17%	14%	3%	21%	3%	24%	18%	17%
120	14%	7%	3%	16%	3%	* 26%	19%	19%
180	16%	15%	2%	20%	3%	25%	19%	19%

Reaction Time (min)	Reaction Temperature: 250 °C							
	Cu	Ni	Pd/C	C	Ru/C	Fe_3O_4	Fe_2O_3	No Catalyst
30	10%	8%	2%	21%	2%	25%	20%	17%
60	9%	3%	3%	15%	1%	24%	17%	16%
90	8%	4%	3%	9%	1%	24%	16%	16%
120	5%	3%	3%	16%	1%	20%	12%	14%
180	5%	1%	3%	15%	1%	9%	12%	14%

After the hydrothermal reduction of AC, it was found that the highest yield of FA was 26% and was obtained by using Fe_3O_4 at 200 °C and 120 min (Table 4).

The maximum value for AA was obtained with Ni, 15% at 250 °C and 180 min. This was followed by that obtained with Cu, 14% at 200 °C and 60 min (Table 5).

Table 5. Yields of acetic acid obtained after the hydrothermal reaction of $\text{NH}_4[\text{H}_2\text{NCO}_2]$ with glucose in the presence of catalysts. The higher yields obtained after the hydrothermal reactions are marked with an asterisk (*).

Reaction Time (min)	Reaction Temperature: 200 °C							
	Cu	Ni	Pd/C	C	Ru/C	Fe_3O_4	Fe_2O_3	No Catalyst
30	9%	9%	6%	7%	9%	11%	11%	11%
60	* 14%	12%	8%	8%	9%	11%	11%	11%
90	11%	12%	8%	11%	8%	11%	11%	12%
120	11%	10%	9%	9%	9%	12%	11%	12%
180	11%	12%	9%	11%	11%	12%	12%	13%

Reaction Time (min)	Reaction Temperature: 250 °C							
	Cu	Ni	Pd/C	C	Ru/C	Fe_3O_4	Fe_2O_3	No Catalyst
30	9%	12%	8%	8%	10%	11%	10%	10%
60	9%	11%	8%	9%	10%	10%	8%	10%
90	10%	13%	9%	6%	11%	11%	11%	11%
120	10%	13%	9%	10%	11%	10%	10%	11%
180	10%	* 15%	10%	11%	13%	11%	10%	11%

Table 6. Yields of lactic acid obtained after the hydrothermal reaction of $\text{NH}_4[\text{H}_2\text{NCO}_2]$ with glucose in the presence of catalysts. The higher yields obtained after the hydrothermal reactions are marked with an asterisk (*).

Reaction Time (min)	Reaction Temperature: 200 °C							
	Cu	Ni	Pd/C	C	Ru/C	Fe_3O_4	Fe_2O_3	No Catalyst
30	8%	9%	5%	* 13%	5%	10%	9%	9%
60	7%	9%	6%	5%	5%	10%	8%	9%
90	10%	8%	4%	11%	3%	* 16%	10%	11%
120	12%	9%	6%	9%	4%	6%	9%	8%
180	9%	9%	6%	7%	5%	5%	10%	10%

Reaction Time (min)	Reaction Temperature: 250 °C							
	Cu	Ni	Pd/C	C	Ru/C	Fe_3O_4	Fe_2O_3	No Catalyst
30	5%	7%	5%	11%	4%	13%	12%	9%
60	8%	4%	4%	11%	4%	6%	9%	10%
90	7%	4%	4%	5%	3%	4%	9%	8%
120	8%	6%	4%	9%	5%	10%	8%	9%
180	6%	5%	4%	10%	3%	10%	8%	10%

For LA, the highest value was 16% and was obtained by using Fe_3O_4 at 200 °C and 90 min. This was followed by that obtained with C, 13% at 200 °C and 30 min (Table 6).

Once again, Fe_3O_4 promoted the maximum yields of FA over AA and LA in comparison to the rest of the catalysts. Only Fe_3O_4 and C improved the yield of FA compared to the sample with no catalyst.

In general, the yields of FA, AA and LA obtained by the reduction of AC are much lower (less than 25%) than those observed with SB (less than 53%). Some other works have shown that sodium bicarbonates and carbonates required high-temperature reactions to achieve higher yields of FA. SB and AC are decomposed easily into HCO_3^- , which is the species that is going to be reduced in the reaction. In the case of AC, not only HCO_3^- is formed. There is another step in which AC is also decomposed because the H^+ protons of the ion NH_4^+ are being donated to other compounds, and then the yield to FA is reduced because there is a competition between two reactions: the reduction of AC and the thermal

decomposition of AC [13,16]. It was observed that the experiments held at 200 °C showed higher yields of FA than the reactions at 250 °C. The reduction of CO₂ is favored by the reaction in alkaline media; when the temperature rises, NH₄⁺ dissociates into NH₃ and H⁺, which are species that reduce the alkalinity and might reduce the solubility of CO₂ in water [10,38].

2.3. Nuclear Magnetic Resonance Spectroscopy Results

It is known that FA can be generated from sugars at lower temperatures in basic aqueous media [32–34] and can be also obtained by the reduction of SB at temperatures higher than 300 °C [29]. In order to understand the reactions, it is necessary to check whether the FA is coming from SB or from glucose and if the catalysts are favoring or disfavoring one or the other reaction. To do so, experiments with an isotope of sodium bicarbonate (NaH¹³CO₃; SB-¹³C) were performed with the different catalysts. ¹³C-NMR analyses were carried out to identify the fraction of formic acid that possesses ¹³C, which comes from the reduction of the carbon source, and the fraction that comes from glucose. The experiments were conducted at 250 °C and 2 h.

The fraction of formic acid coming from the SB-¹³C when using each of the catalysts is presented in Figure 2.

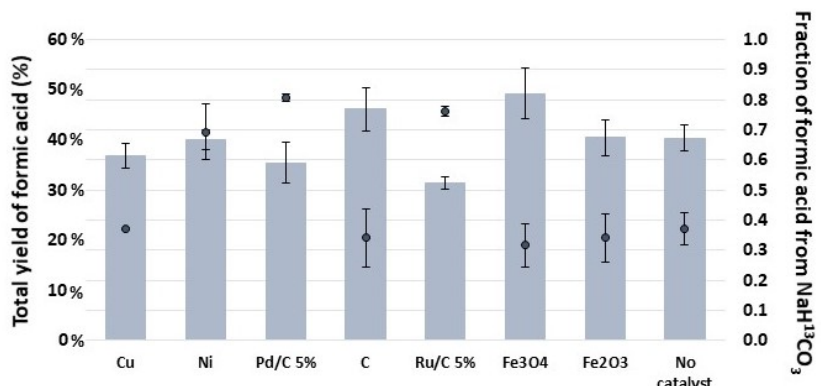


Figure 2. Fractions of formic acid coming from the reduction NaH¹³CO₃ and from the oxidation of glucose for each of the catalysts at 250 °C and 2 h. Gray bars represent the total yield of formic acid of each sample (obtained by HPLC); black dots represent the fraction of formic acid coming from NaH¹³CO₃ (obtained by ¹³C-NMR). The average error in the measure of the fraction of formic acid was 5%.

It was observed that although Fe₃O₄ is the catalyst that provides the highest yield of total FA (49%, 250 °C and 2h, measured by HPLC), its proportion of reduced SB-¹³C is lower (0.32) in comparison to the fraction of FA obtained with Pd/C 5%, Ru/C 5% and Ni (0.81, 0.76 and 0.69, respectively).

The metal supported catalysts (Pd/C 5% and Ru/C 5%) presented the highest selectivity in reducing CO₂ in comparison to the performance of the activated carbon support (C), which reached a fraction of 0.34.

There were catalysts that did not improve the reduction of SB-¹³C; in fact, the reaction without catalyst (fraction FA-¹³C: 0.37) showed a slightly higher capability to reduce CO₂ than Cu, Fe₃O₄ and Fe₂O₃ (0.37, 0.32 and 0.34, respectively).

The order in which catalysts were able to reduce CO₂ captured as SB-¹³C was as follows: Pd/C 5% > Ru/C 5% > Ni > Cu > C ≈ Fe₂O₃ > Fe₃O₄.

In all the experiments, the only products that came from the direct reduction of carbon source (SB-¹³C) were FA-¹³C at δ = 163 ppm and an unidentified compound at δ = 173 ppm (this peak was absent in Fe₂O₃ and in the sample with no catalyst). At δ = 127 ppm, another peak was observed; according to the literature [39,40], this compound could be ¹³CO₂ dissolved in the sample.

An AA-¹³C standard was injected. AA-¹³C standard peak was observed at $\delta = 184$ ppm, and then the possibility that the unidentified peak at $\delta = 173$ ppm was AA-¹³C was excluded.

Possible Mechanisms of Reaction

In the NMR spectra, it was confirmed that the reduction of the carbon source led mostly to the formation of FA, while byproducts and FA were obtained from the oxidation of glucose.

In literature were found some of the possible mechanisms of reaction of glucose at high water temperatures, subcritical and supercritical water [41–44]. Glucose can be transformed in two different ways: by following a retro-aldol condensation reaction to produce glycolaldehyde or through the isomerization of the glucose into fructose (favored by basic media) which can be dehydrated to form 5-HMF (favored by the acid media) or can produce glyceraldehyde by means of another retro-aldol condensation reaction. Finally, the glyceraldehyde can be isomerized into pyruvaldehyde, which could be a precursor of lactic acid.

Besides the retro-aldol reactions that can lead to the production of lactic acid and glycolaldehyde, 5-HMF can be transformed into formaldehyde and furfural in acid media [43], but in our case, reactions were performed in basic media, so this step may or may not be occurring.

Some other works [42] described that glucose can also dehydrate to form 1,6-anhydroglucose. This molecule can be a precursor of acids or can be transformed into D-fructose and follow a reverse aldol condensation reaction to form erythrose and glycolaldehyde that can produce acids as well. In Figure 3, the main mechanisms of oxidation of glucose are represented. According to Kabyemela et al. [42], some of the products derived from the oxidation of glucose that can be identified according to these mechanisms are fructose, erythrose, glyceraldehyde, glycolaldehyde, pyruvaldehyde, dihydroxyacetone, 1,6-anhydroglucose, 5-HMF, acetic acid and formic acid. Kabyemela et al. [42] also have identified some products of the decomposition of fructose such as pyruvaldehyde, erythrose, glyceraldehyde, dihydroxyacetone, acetic acid and formic acid. Erythrose and 1,6-anhydroglucose can also be the precursors of acetic and formic acids.

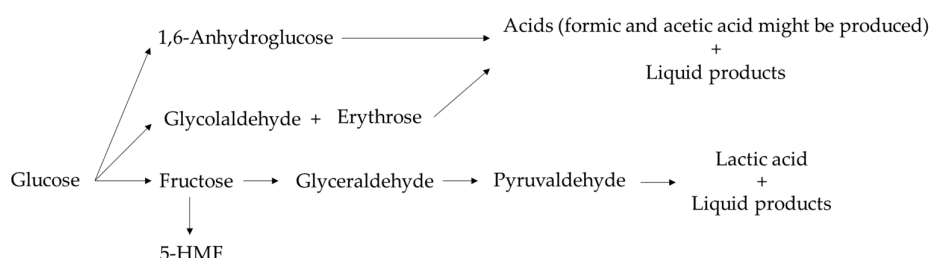


Figure 3. Mechanisms of oxidation of glucose.

Glucose has five -OH (hydroxyl) groups. In a previous work, it has been proposed that alcohol groups act as reducing agents for CO₂ [29]. According to Shen et al., the reduction of the carbon source is mainly due to the alcohol moiety [8,45]. According to other studies, compounds with primary alcohol groups presented slightly higher yields in comparison with compounds with secondary alcohol groups. Because of the steric effects, the position of the hydroxyl group in the compound could be of importance in the reduction of the carbon source [29]. Shen et al. proposed a mechanism of reduction of CO₂ through alcohol molecules in which, through a cyclic transition state, a H[−] from the α -carbon of −OH moiety is transferred to the ion bicarbonate and the resulting species dehydrate quickly into formate [8,29,45]. Most of the products of glucose decomposition contain alcohol groups (fructose, glyceraldehyde, glycolaldehyde, lactic acid), and Andérez et al. [29] proved that formic acid is rendered in appreciable yields.

Regarding catalysts, it can be found in the literature that in reactions that use metals as reductants, HCO_3^- is adsorbed on a Pd/C surface, promoting the formation of C_1 intermediates species to produce FA and traces of CH_4 and improving the generation of C-C bonds to form C_2 compounds [46]. Cu and Ni have showed also good performance in reducing HCO_3^- into C_1 compounds when using metals such as Fe as reducing agents [47,48]. In other studies, experiments with a mix of Fe and Fe_3O_4 were performed to reduce CO_2 . In these works, Fe is reduced into Fe_3O_4 , generating hydrogen. Fe_3O_4 is transformed into $\text{Fe}_{3-x}\text{O}_4$, and then hydrogen and $\text{C}=\text{O}$ of HCO_3^- are adsorbed in the surface of the metal oxide and react to produce formic acid [49].

As seen before, catalysts can influence the performance of the hydrothermal reactions for CO_2 reduction and glucose oxidation.

3. Materials and Methods

3.1. Chemicals

Ammonium carbamate (AC) (99%), sodium bicarbonate (SB) (100%), sodium bicarbonate ^{13}C (SB- ^{13}C) (100%) and acetic acid ^{13}C (AA- ^{13}C) were used as sources of captured CO_2 . D-(+)-Glucose (100%) was used as reducing agent. Fine powder of commercial Cu, Ni, Pd/C (5 wt% of metal loading), activated carbon, Ru/C (5 wt% of metal loading, 50% water wet paste), Fe_2O_3 and Fe_3O_4 were used as catalysts. Sodium bicarbonate was purchased from COFARCAS (Spain), Ru/c 5% was provided by Strem Chemicals and the rest of the chemicals were acquired from Sigma-Aldrich. Deionized water was used to prepare the dilutions.

3.2. Catalytic Experiments

Two solutions were prepared: the first one contained 0.05 M of glucose and 0.5 M of sodium bicarbonate, and the second one consisted of 0.05 M glucose and 0.5 M ammonium carbamate (ratio 1:10, glucose:carbon source in mol). Hydrothermal reactions for the conversion of CO_2 (captured as ammonium carbamate and sodium bicarbonate) were carried out in SS316 stainless steel horizontal tubular reactors of 10 mL (internal volume). The batch reactors were filled with liquid up to 45% of the total volume.

Different sets of reactions were performed at temperatures of 200 and 250 °C for 30, 60, 90, 120 and 180 min. The pressure inside the reactor corresponds to the saturation pressure of the set temperature. A fluidized bed heater was used to reach the temperature of the reactions. A temperature probe was installed inside the vessels. Reactors were placed in the heaters, achieving the working temperature within 7 min. Once the residence time was completed, each reactor was immediately extracted and placed in a bath of cold water. All samples were filtered with 0.22 μm Nylon filter and then collected in glass vials to be analyzed by HPLC or NMR spectroscopy.

The yields to formic acid, lactic acid and acetic acid were calculated as follows:

$$Y_{\text{product}} = \frac{C_{\text{Product},f}}{C_{\text{Glucose},i}} \quad (1)$$

where $C_{\text{Product},f}$ is the molar concentration of formic acid at the end of the reaction and $C_{\text{Glucose},i}$ is the initial molar concentration of glucose.

All the experiments were repeated at least 2 times, and the error was calculated with the standard deviations of the yields.

The amounts of catalyst used were as follows: For Cu and Ni, a molar relation of metal:carbon source of 5:1 was used. For Pd/C 5%, C and Ru/C 5%, 55 wt% catalyst with respect to the initial weight of carbon source was added. For Fe_3O_4 and Fe_2O_3 , a molar relation of metal:carbon source of 1:1 was utilized.

3.3. Scanning Electronic Microscopy (SEM)

SEM images of the catalyst were taken in order to corroborate the particle size. An FEI QUANTA 200 FEG (ESEM) was used at high-vacuum operation ($<6 \times 10^{-4}$ Pa (4.5×10^{-2} Torr)), electron landing energy of 5 keV and spot of 3.0.

3.4. High-Pressure Liquid Chromatography (HPLC)

The liquid samples were analyzed by HPLC (Waters, Alliance separation module e2695) with RI detector (Waters, 2414 module) and a Rezex ROA-Organic Acid H+ (8%) column. As mobile phase, 25 mM H₂SO₄ was used at 0.5 mL/min of flow rate. The temperatures of the column and the detector were 40 and 30 °C.

3.5. Nuclear Magnetic Resonance Spectroscopy (NMR Spectroscopy)

Spectra of all the samples in which SB-¹³C was used as carbon source were recorded on a 500 MHz Agilent instrument equipped with a OneNMR probe. The acquisition parameters for ¹³C NMR spectra were as follows: 25 °C, 70 s relaxation delay between transients, 45° pulse width, spectral width of 31250 Hz, a total of 16 transients and 1.048 s acquisition time. The inverse gated decoupling technique to suppress the nuclear Overhauser effect (NOE) was used to obtain quantitative measurement. The acquisition parameters for ¹H NMR spectra were as follows: 25 °C, 70 s relaxation delay between transients, 90° pulse width, spectral width of 8012.8 Hz, a total of 4 transients and 2.044 s acquisition time. The sequence PRESAT was used in order to suppress the strong signal of water.

¹H and ¹³C NMR chemical shifts (δ) were reported in parts per million (ppm) and referenced to tetramethylsilane (TMS).

4. Conclusions

In this work, the hydrothermal conversion of CO₂ captured as sodium bicarbonate and ammonium carbamate was studied. Glucose was used as a reducing agent, and metal and metal oxides (Cu, Ni, Pd/C 5%, Ru/C 5%, Fe₂O₃ and Fe₃O₄), as well as activated carbon (C), were used as catalysts. The main products of the reaction with ammonium carbamate were formic acid, acetic acid and lactic acid.

The yields of formic acid, acetic acid and lactic acid obtained by the reduction of ammonium carbamate were much lower (less than 25%) than those observed when sodium bicarbonate was used as the carbon source (less than 53%).

For ammonium carbamate experiments, C and Fe₃O₄ promoted higher yields of FA over AA and LA in comparison to the rest of the catalysts and improved the yield of FA in comparison to the sample without catalyst.

In the experiments with sodium bicarbonate, C and Fe₃O₄ appeared to be the most promising catalysts for improving the yield of formic acid. The origin of the carbon forming formic acid was investigated by using NaH¹³CO₃. It was found that although C and Fe₃O₄ achieved the highest total formic acid yield, they seem to favor the oxidation of glucose instead of the reduction of CO₂. However, it should be noted that even though Pd/C 5%, Ni and Ru/C 5% yields of total formic acid were lower, they were shown to be more selective in producing formic acid from CO₂ than the other catalysts. This aspect is important when considering the selection of a catalyst for making a process that primarily promotes a higher conversion of the carbon source.

Author Contributions: Conceptualization, M.D.B., F.A.M., Á.M. and M.I.C.; methodology, M.D.B. and M.I.C.; formal analysis, M.I.C.; investigation, M.D.B. and M.I.C.; resources, M.D.B., F.A.M., Á.M. and M.I.C.; writing—original draft preparation, M.D.B. and M.I.C.; supervision, M.D.B., F.A.M. and Á.M.; funding acquisition, M.D.B. and Á.M. All authors have read and agreed to the published version of the manuscript.

Funding: This research was funded by Ministerio de Ciencia y Universidades by project RTI2018-097456-B-I00 and by the Regional Government of Castilla y León and the EU-FEDER program (CLU-2019-04).

Institutional Review Board Statement: Not applicable.

Informed Consent Statement: Not applicable.

Acknowledgments: M.I.C. acknowledges Universidad de Valladolid and Banco de Santander for the predoctoral grant. The authors acknowledge Laboratorio de Técnicas Instrumentales UVa for their assistance in the NMR and SEM analysis.

Conflicts of Interest: The authors declare no conflict of interest.

References

1. Intergovernmental Panel on Climate Change Global Warming of 1.5 °C. Available online: <https://www.ipcc.ch/sr15/> (accessed on 21 December 2021).
2. United Nations el Acuerdo de París | CMNUCC. Available online: <https://unfccc.int/es/process-and-meetings/the-paris-agreement/el-acuerdo-de-paris> (accessed on 27 January 2022).
3. Khezri, M.; Heshmati, A.; Khodaei, M. Environmental Implications of Economic Complexity and Its Role in Determining How Renewable Energies Affect CO₂ Emissions. *Appl. Energy* **2022**, *306*, 117948. [\[CrossRef\]](#)
4. Tapia, J.F.D.; Lee, J.Y.; Ooi, R.E.H.; Foo, D.C.Y.; Tan, R.R. A Review of Optimization and Decision-Making Models for the Planning of CO₂ Capture, Utilization and Storage (CCUS) Systems. *Sustain. Prod. Consum.* **2018**, *13*, 1–15. [\[CrossRef\]](#)
5. Sakakura, T.; Choi, J.C.; Yasuda, H. Transformation of Carbon Dioxide. *Chem. Rev.* **2007**, *107*, 2365–2387. [\[CrossRef\]](#) [\[PubMed\]](#)
6. Dibenedetto, A.; Angelini, A.; Stufano, P. Use of Carbon Dioxide as Feedstock for Chemicals and Fuels: Homogeneous and Heterogeneous Catalysis. *J. Chem. Technol. Biotechnol.* **2014**, *89*, 334–353. [\[CrossRef\]](#)
7. Rafiee, A.; Rajab Khalilpour, K.; Milani, D.; Panahi, M. Trends in CO₂ Conversion and Utilization: A Review from Process Systems Perspective. *J. Environ. Chem. Eng.* **2018**, *6*, 5571–5794. [\[CrossRef\]](#)
8. Shen, Z.; Zhang, Y.; Jin, F. The Alcohol-Mediated Reduction of CO₂ and NaHCO₃ into Formate: A Hydrogen Transfer Reduction of NaHCO₃ with Glycerine under Alkaline Hydrothermal Conditions. *RSC Adv.* **2012**, *2*, 797–801. [\[CrossRef\]](#)
9. Mikkelsen, M.; Jørgensen, M.; Krebs, F.C. The Teraton Challenge. A Review of Fixation and Transformation of Carbon Dioxide. *Energy Environ. Sci.* **2010**, *3*, 43–81. [\[CrossRef\]](#)
10. He, C.; Tian, G.; Liu, Z.; Feng, S. A Mild Hydrothermal Route to Fix Carbon Dioxide to Simple Carboxylic Acids. *Org. Lett.* **2010**, *12*, 649–651. [\[CrossRef\]](#)
11. Fouustoukos, D.I.; Seyfried, W.E. Hydrocarbons in Hydrothermal Vent Fluids: The Role of Chromium-Bearing Catalysts. *Science* **2004**, *304*, 1002–1005. [\[CrossRef\]](#)
12. del Río, J.I.; Pérez, E.; León, D.; Martín, Á.; Bermejo, M.D. Catalytic Hydrothermal Conversion of CO₂ Captured by Ammonia into Formate Using Aluminum-Sourced Hydrogen at Mild Reaction Conditions. *J. Ind. Eng. Chem.* **2021**, *97*, 539–548. [\[CrossRef\]](#)
13. Etiope, G.; Sherwood Lollar, B. Abiotic Methane on Earth. *Rev. Geophys.* **2013**, *51*, 276–299. [\[CrossRef\]](#)
14. Centi, G.; Quadrelli, E.A.; Perathoner, S. Catalysis for CO₂ Conversion: A Key Technology for Rapid Introduction of Renewable Energy in the Value Chain of Chemical Industries. *Energy Environ. Sci.* **2013**, *6*, 1711–1731. [\[CrossRef\]](#)
15. Ahn, C.K.; Lee, H.W.; Lee, M.W.; Chang, Y.S.; Han, K.; Rhee, C.H.; Kim, J.Y.; Chun, H.D.; Park, J.M. Determination of Ammonium Salt/Ion Speciation in the CO₂ Absorption Process Using Ammonia Solution: Modeling and Experimental Approaches. *Energy Procedia* **2011**, *4*, 541–547. [\[CrossRef\]](#)
16. Uhm, S.; Chung, S.T.; Lee, J. Characterization of Direct Formic Acid Fuel Cells by Impedance Studies: In Comparison of Direct Methanol Fuel Cells. *J. Power Sources* **2008**, *178*, 34–43. [\[CrossRef\]](#)
17. Rice, C.; Ha, S.; Masel, R.I.; Waszczuk, P.; Wieckowski, A.; Barnard, T. Direct Formic Acid Fuel Cells. *J. Power Sources* **2002**, *111*, 83–89. [\[CrossRef\]](#)
18. Roman-Gonzalez, D.; Moro, A.; Burgoa, F.; Pérez, E.; Nieto-Márquez, A.; Martín, Á.; Bermejo, M.D. 2Hydrothermal CO₂ Conversion Using Zinc as Reductant: Batch Reaction, Modeling and Parametric Analysis of the Process. *J. Supercrit. Fluids* **2018**, *140*, 320–328. [\[CrossRef\]](#)
19. Duo, J.; Jin, F.; Wang, Y.; Zhong, H.; Lyu, L.; Yao, G.; Huo, Z. NaHCO₃-Enhanced Hydrogen Production from Water with Fe and in Situ Highly Efficient and Autocatalytic NaHCO₃ Reduction into Formic Acid. *Chem. Commun.* **2016**, *52*, 3316–3319. [\[CrossRef\]](#)
20. Jin, F.; Gao, Y.; Jin, Y.; Zhang, Y.; Cao, J.; Wei, Z.; Smith, R.L. High-Yield Reduction of Carbon Dioxide into Formic Acid by Zero-Valent Metal/Metal Oxide Redox Cycles. *Energy Environ. Sci.* **2011**, *4*, 881–884. [\[CrossRef\]](#)
21. Lyu, L.; Jin, F.; Zhong, H.; Chen, H.; Yao, G. A Novel Approach to Reduction of CO₂ into Methanol by Water Splitting with Aluminum over a Copper Catalyst. *RSC Adv.* **2015**, *5*, 31450–31453. [\[CrossRef\]](#)
22. Takahashi, H.; Kori, T.; Onoki, T.; Tohji, K.; Yamasaki, N. Hydrothermal Processing of Metal Based Compounds and Carbon Dioxide for the Synthesis of Organic Compounds. *J. Mater. Sci.* **2008**, *43*, 2487–2491. [\[CrossRef\]](#)
23. Zhong, H.; Yao, G.; Cui, X.; Yan, P.; Wang, X.; Jin, F. Selective Conversion of Carbon Dioxide into Methane with a 98% Yield on an In Situ Formed Ni Nanoparticle Catalyst in Water. *Chem. Eng. J.* **2019**, *357*, 421–427. [\[CrossRef\]](#)
24. Chen, Y.; Jing, Z.; Miao, J.; Zhang, Y.; Fan, J. Reduction of CO₂ with Water Splitting Hydrogen under Subcritical and Supercritical Hydrothermal Conditions. *Int. J. Hydrogen Energy* **2016**, *41*, 9123–9127. [\[CrossRef\]](#)

25. Le, Y.; Yao, G.; Zhong, H.; Jin, B.; He, R.; Jin, F. Rapid Catalytic Reduction of NaHCO_3 into Formic Acid and Methane with Hydrazine over Raney Ni Catalyst. *Catal. Today* **2017**, *298*, 124–129. [\[CrossRef\]](#)

26. Chen, Q.; Qian, Y. Carbon Dioxide Thermal System: An Effective Method for the Reduction of Carbon Dioxide. *Chem. Commun.* **2001**, 1402–1403. [\[CrossRef\]](#)

27. Su, J.; Lu, M.; Lin, H. High Yield Production of Formate by Hydrogenating CO_2 Derived Ammonium Carbamate/Carbonate at Room Temperature. *Green Chem.* **2015**, *17*, 2769–2773. [\[CrossRef\]](#)

28. Farnetti, E.; Crotti, C. Selective Oxidation of Glycerol to Formic Acid Catalyzed by Iron Salts. *Catal. Commun.* **2016**, *84*, 1–4. [\[CrossRef\]](#)

29. Andérez-Fernández, M.; Pérez, E.; Martín, A.; Bermejo, M.D. Hydrothermal CO_2 Reduction Using Biomass Derivatives as Reductants. *J. Supercrit. Fluids* **2018**, *133*, 658–664. [\[CrossRef\]](#)

30. Kang, S.; Li, X.; Fan, J.; Chang, J. Hydrothermal Conversion of Lignin: A Review. *Renew. Sustain. Energy Rev.* **2013**, *27*, 546–558. [\[CrossRef\]](#)

31. Jin, F.; Zeng, X.; Jing, Z.; Enomoto, H. A Potentially Useful Technology by Mimicking Nature—Rapid Conversion of Biomass and CO_2 into Chemicals and Fuels under Hydrothermal Conditions. *Ind. Eng. Chem. Res.* **2012**, *51*, 9921–9937. [\[CrossRef\]](#)

32. Yun, J.; Yao, G.; Jin, F.; Zhong, H.; Kishita, A.; Tohji, K.; Enomoto, H.; Wang, L. Low-Temperature and Highly Efficient Conversion of Saccharides into Formic Acid under Hydrothermal Conditions. *AIChE J.* **2016**, *62*, 3657–3663. [\[CrossRef\]](#)

33. Sundqvist, B.; Karlsson, O.; Westermark, U. Determination of Formic-Acid and Acetic Acid Concentrations Formed during Hydrothermal Treatment of Birch Wood and Its Relation to Colour, Strength and Hardness. *Wood Sci. Technol.* **2006**, *40*, 549–561. [\[CrossRef\]](#)

34. Gao, P.; Li, G.; Yang, F.; Lv, X.N.; Fan, H.; Meng, L.; Yu, X.Q. Preparation of Lactic Acid, Formic Acid and Acetic Acid from Cotton Cellulose by the Alkaline Pre-Treatment and Hydrothermal Degradation. *Ind. Crops Prod.* **2013**, *48*, 61–67. [\[CrossRef\]](#)

35. Ding, K.; Le, Y.; Yao, G.; Ma, Z.; Jin, B.; Wang, J.; Jin, F. A Rapid and Efficient Hydrothermal Conversion of Coconut Husk into Formic Acid and Acetic Acid. *Process Biochem.* **2018**, *68*, 131–135. [\[CrossRef\]](#)

36. Cantero, D.A.; Vaquerizo, L.; Martinez, C.; Bermejo, M.D.; Cocero, M.J. Selective Transformation of Fructose and High Fructose Content Biomass into Lactic Acid in Supercritical Water. *Catal. Today* **2015**, *255*, 80–86. [\[CrossRef\]](#)

37. Cantero, D.A.; Bermejo, M.D.; Cocero, M.J. Kinetic Analysis of Cellulose Depolymerization Reactions in near Critical Water. *J. Supercrit. Fluids* **2013**, *75*, 48–57. [\[CrossRef\]](#)

38. Takahashi, H.; Liu, L.H.; Yashiro, Y.; Ioku, K.; Bignall, G.; Yamasaki, N.; Kori, T. CO_2 Reduction Using Hydrothermal Method for the Selective Formation of Organic Compounds. *J. Mater. Sci.* **2006**, *41*, 1585–1589. [\[CrossRef\]](#)

39. Ethier, A.L.; Switzer, J.R.; Rumble, A.C.; Medina-Ramos, W.; Li, Z.; Fisk, J.; Holden, B.; Gelbaum, L.; Pollet, P.; Eckert, C.A.; et al. The Effects of Solvent and Added Bases on the Protection of Benzylamines with Carbon Dioxide. *Processes* **2015**, *3*, 497–513. [\[CrossRef\]](#)

40. Merritt, M.E.; Harrison, C.; Storey, C.; Jeffrey, F.M.; Sherry, A.D.; Malloy, C.R. Hyperpolarized ^{13}C Allows a Direct Measure of Flux through a Single Enzyme-Catalyzed Step by NMR. *Proc. Natl. Acad. Sci. USA* **2007**, *104*, 19773–19777. [\[CrossRef\]](#)

41. Aida, T.M.; Sato, Y.; Watanabe, M.; Tajima, K.; Nonaka, T.; Hattori, H.; Arai, K. Dehydration of D-Glucose in High Temperature Water at Pressures up to 80 MPa. *J. Supercrit. Fluids* **2007**, *40*, 381–388. [\[CrossRef\]](#)

42. Kabyemela, B.M.; Adschari, T.; Malaluan, R.M.; Arai, K. Glucose and Fructose Decomposition in Subcritical and Supercritical Water: Detailed Reaction Pathway, Mechanisms, and Kinetics. *Ind. Eng. Chem. Res.* **1999**, *38*, 2888–2895. [\[CrossRef\]](#)

43. Sasaki, M.; Goto, K.; Tajima, K.; Adschari, T.; Arai, K. Rapid and Selective Retro-Aldol Condensation of Glucose to Glycolaldehyde in Supercritical Water. *Green Chem.* **2002**, *4*, 285–287. [\[CrossRef\]](#)

44. Cantero, D.A.; Álvarez, A.; Bermejo, M.D.; Cocero, M.J. Transformation of Glucose into Added Value Compounds in a Hydrothermal Reaction Media. *J. Supercrit. Fluids* **2015**, *98*, 204–210. [\[CrossRef\]](#)

45. Shen, Z.; Zhang, Y.; Jin, F. From NaHCO_3 into Formate and from Isopropanol into Acetone: Hydrogen-Transfer Reduction of NaHCO_3 with Isopropanol in High-Temperature Water. *Green Chem.* **2011**, *13*, 820–823. [\[CrossRef\]](#)

46. Zhong, H.; Yao, H.; Duo, J.; Yao, G.; Jin, F. Pd/C-Catalyzed Reduction of NaHCO_3 into CH_3COOH with Water as a Hydrogen Source. *Catal. Today* **2016**, *274*, 28–34. [\[CrossRef\]](#)

47. Kudo, K.; Komatsu, K. Selective Formation of Methane in Reduction of CO_2 with Water by Raney Alloy Catalyst. *J. Mol. Catal. A Chem.* **1999**, *145*, 257–264. [\[CrossRef\]](#)

48. Zhong, H.; Gao, Y.; Yao, G.; Zeng, X.; Li, Q.; Huo, Z.; Jin, F. Highly Efficient Water Splitting and Carbon Dioxide Reduction into Formic Acid with Iron and Copper Powder. *Chem. Eng. J.* **2015**, *280*, 215–221. [\[CrossRef\]](#)

49. Liu, X.; Zhong, H.; Wang, C.; He, D.; Jin, F. CO_2 Reduction into Formic Acid under Hydrothermal Conditions: A Mini Review. *Energy Sci. Eng.* **2022**, *1*–13. [\[CrossRef\]](#)